ELectronics EXpress

IEICE Electronics Express, Vol.8, No.5, 291–298

Characterization of a MEMS resonator with extended hysteresis

Suketu Naik[a)] **and Takashi Hikihara**

Department of Electrical Engineering,
Kyoto University, Katsura, Nishikyo,
Kyoto, 615–8510, Japan

a) *naik@dove.kuee.kyoto-u.ac.jp*

Abstract: In this paper an electrostatically driven MEMS resonator with resonance and hysteresis characteristics is reported. The resonator begins to exhibit spring-hardening effect at ac excitation voltage of 105 mV and dc bias voltage of 5 V in vacuum at 50 Pa. An extended hysteresis at low pressure and high excitation voltage during upsweep and downsweep of excitation frequency was observed. This characteristic facilitates the usage of this type of resonator in a range of applications such as a cascaded filter array or as a high bandwidth resonator.

Keywords: MEMS resonator, spring-hardening effect, hysteresis
Classification: Micro- or nano-electromechanical systems

References

[1] A. Partridge and J. McDonald, "MEMS to replace quartz oscillators as frequency sources," *NASA Technical Brief*, vol. 30, no. 6, 2006.
[2] L. Yan, et. al., "A 1.14 GHz piezoelectrically transduced disk resonator," *18th IEEE Int. Conf. MEMS*, pp. 203–206, 2005.
[3] V. Kaajakari, et. al., "Nonlinear limits for single-crystal silicon microresonators," *J. MEMS*, vol. 13, no. 5, pp. 715–724, 2004.
[4] R. M. C. Mestrom, et. al., "Nonlinear oscillations in MEMS resonators," *Sensors and Actuators A*, vol. 142, no. 1, pp. 306–315, 2008.
[5] S. Beeby, *MEMS Mechanical Sensors*, Artech House Publishers, Norwood, 2004.
[6] C. T.-C. Nguyen, et. al., "An integrated CMOS micromechanical resonator high-Q oscillator," *IEEE J. Solid-State Circuits*, vol. 34, no. 4, pp. 440–455, 1999.
[7] D. Miki, et. al., "Large-Amplitude MEMS Electret Generator with Nonlinear Spring," *23rd IEEE Int. Conf. Microw. Electron. Mechanical Syst.*, pp. 176–179, 2010.
[8] L. Oropeza-Ramos, et. al., "Robust micro-rate sensor actuated by parametric resonance," *Sensors and Actuators A*, vol. 152, pp. 80–87, 2009.
[9] A. Cowen, et. al., *SOIMUMPs Design Handbook revision 6.0*, MEMSCAP, Inc., Research Triangle Park, 2009.
[10] C. Acar and A. Shkel, *MEMS Vibratory Gyroscopes*, Springer Science+Business Media, New York, 2009.

DOI: 10.1587/elex.8.291
Received January 26, 2011
Accepted February 01, 2011
Published March 10, 2011

[11] 4294A Impedance analyzer service manual.
[Online] http://home.agilent.com

1 Introduction

With the maturation of MEMS technology, MEMS resonators are being substituted for crystal oscillators and for high-Q oscillator references [1, 2]. A MEMS resonator is limited to a maximum usable amplitude at its resonance frequency. Past a specific amplitude, the frequency peak shifts from linear resonance to nonlinear resonance. Usually nonlinear effect is characterized and the device is operated below the corresponding amplitude to adhere to predictable performance parameters [3]. At a higher vibration amplitude, the device may exhibit hysteresis during upsweep and downsweep of frequency. The causes of hysteresis in MEMS resonators include material anisotropicity in a nonuniform material, large vibrations, variation in individual structure elements during fabrication, circuit elements, and/or a combination of all of the above. In particular spring-hardening effect in electrostatically excited fixed-fixed beam resonator and comb-drive resonator has already been reported in MEMS research [4, 5, 6]. Along with excitation voltage and bias voltage, actuation mechanisms such as parallel plate comb-drive or laterally driven comb-drive can determine whether spring-softening or spring-hardening behavior is exhibited. In [7] a MEMS energy harvesting device excited by mechanical vibration was characterized with spring-hardening effect creating an extension of 27 Hz. In [8] parametric resonance was exploited to show that the spring-hardening effect can extend the resonance curve up to 1 kHz. In this work, we show a laterally driven comb-drive resonator that can, a) extend its hysteresis range, and b) maintain its high amplitude vibration under proper excitation conditions. The width of the hysteresis which is determined from the two jump points during upsweep and downsweep is the key to understanding the synchronized behavior of coupled resonators; this aspect is particularly beneficial in our ongoing research work. Consequently a resonator with an extended hysteresis has an obvious advantage of switching between high and low amplitude states. In this paper, experimental results of a MEMS resonator with spring-hardening effect with an extended hysteresis are summarized.

2 Resonator design

Devices were fabricated in SOIMUMPs [9] in which 25 μm thick silicon is used as the structure layer. The substrate underneath the structure is completely removed in a back-etch which reduces parasitic capacitances and damping. The resonator consists of a perforated mass suspended by folded beams with a ratio as shown in Fig. 1a. The springs are attached to a truss. The device is designed to be symmetric about x and y axes to provide stable oscillations. Important dimensions and features of the device are as follows: the lengths

DOI: 10.1587/elex.8.291
Received January 26, 2011
Accepted February 01, 2011
Published March 10, 2011

of outer beam and inner beam are 306 μm and 331 μm respectively, number of movable fingers=39, gap between movable and fixed fingers=3 μm, spring area=3 μm × 285 μm, and mass area=175 μm × 575 μm. The device is actuated by applying an ac voltage with a dc bias voltage between the mass and either of the electrodes. The device is designed to vibrate only in x-direction due to specific design features such as folded beams, truss and a high aspect ratio. Typically the motional current, which is proportional to the change in the capacitance between the comb fingers and the excitation voltage, is measured.

3 Measurement results and discussion

Measurements were performed on Agilent 4294A impedance analyzer using the test setup shown in Fig. 1b. The impedance of the Device Under Test (DUT), is measured by calculating the ratio between the voltage across the DUT and the current across it, consisting of magnitude and phase [11]. For all measurements shown in this paper, left electrode (see Fig. 1a) was connected to the high port, anchor was connected to the low port of the impedance analyzer, and right electrode was connected to ground. Using capacitive bridge technique impedance analyzer utilizes ac voltage + dc bias as an excitation voltage and determines the impedance based on the current produced by the device which is measured from the low port. For all the measurements shown in the subsequent sections, the data contains real part and imaginary part of complex impedance. By selecting this option impedance analyzer calculates equivalent series resistance as the real part and equivalent series reactance as the imaginary part. From equivalent circuit model of a resonator, the real part contains a purely mechanical term and an offset added by purely ca-

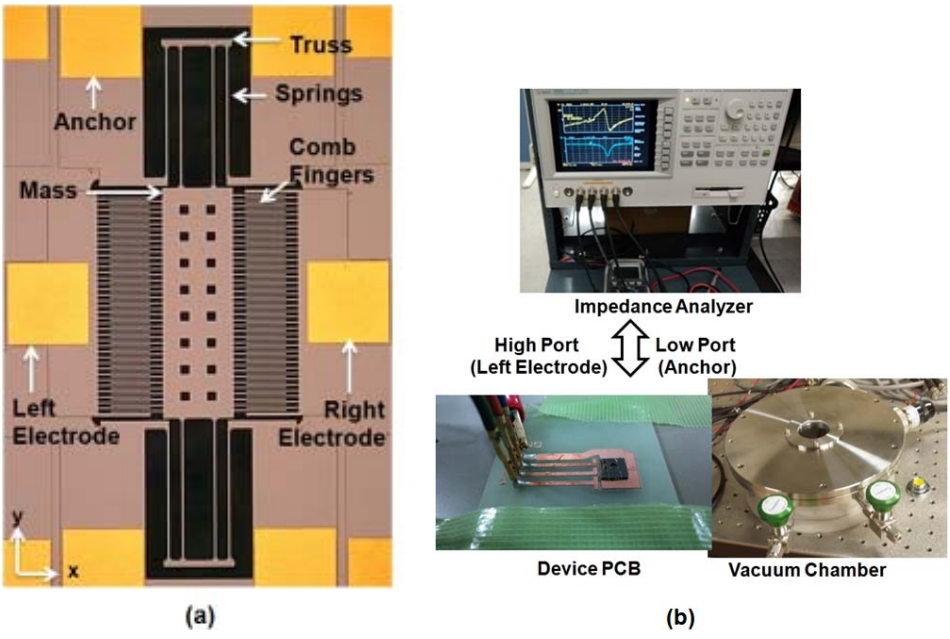

Fig. 1. (a) Fabricated device and (b) test setup used in the experiments.

DOI: 10.1587/elex.8.291
Received January 26, 2011
Accepted February 01, 2011
Published March 10, 2011

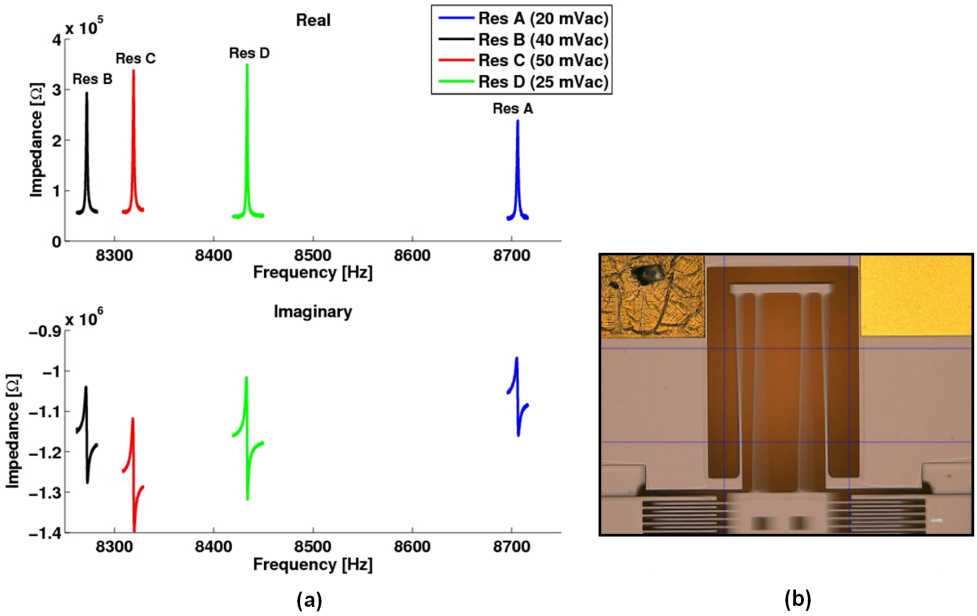

Fig. 2. Resonance: (a) response curves of four resonators at 50 Pa and dc bias=20 V and (b) resonator A in motion at resonance frequency.

pacitive term, whereas the imaginary part contains purely capacitive terms. Thus, the mechanical and electrical parameters can be quickly observed from this data.

3.1 Resonance characteristics

Fig. 2a shows the frequency response curves of four resonators on separate dies labeled as Res A, Res B, Res C, and Res D. The resonators were excited at same dc bias but at different ac excitation voltage so that they can operate linearly. Fig. 2b shows Res A in motion around its resonance frequency. The imaginary part of the curves at the bottom shows the change in overall capacitance as the excitation frequency is swept. Based on the maximum value of the real part of the curves, the resonance frequencies were calculated as 8.706 kHz for Res A, 8.272 kHz for Res B, 8.319 kHz for Res C, and 8.434 kHz for Res D. Taking the resonance frequency of Res C as the center, variation of other resonance frequencies were calculated as 4.65% for Res A, 0.57% for Res B, and 1.38% for Res D. This can be due to variation in the effective mass on different dies during fabrication. Other causes of variation include different doping angle, debris deposited during fabrication and die separation, minute cracks, and/or change in parasitic capacitance of bonding wires and circuit board. Although the excitation voltage plays a role damping is different in the four resonators. From –3 dB bandwidth points around the resonance frequency Q was calculated as 3913 for Res A, 4412 for Res B, 4687 for Res C, and 6423 for Res D.

DOI: 10.1587/elex.8.291
Received January 26, 2011
Accepted February 01, 2011
Published March 10, 2011

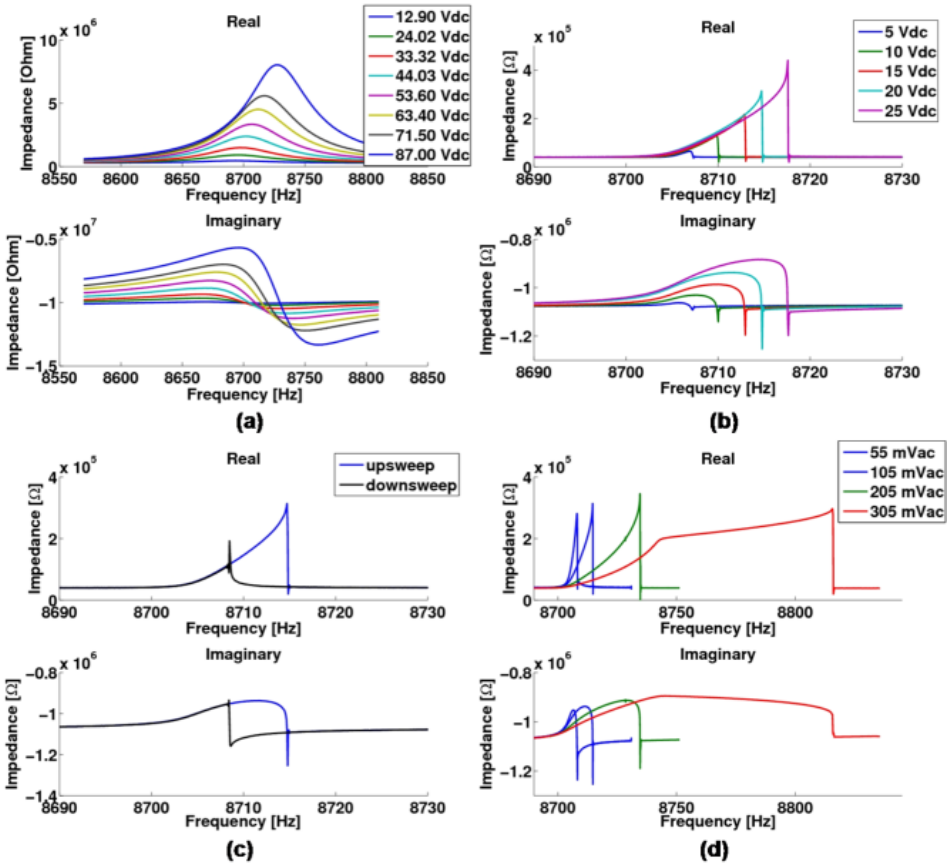

Fig. 3. Frequency response curves of one of resonators: (a) dc bias sweep in air with ac voltage=1 V, (b) dc bias sweep in vacuum (50 Pa) with ac voltage=105 mV, (c) Hysteresis in vacuum (50 Pa) with ac voltage=105 mV, dc bias=20 V, and (d) ac voltage sweep in vacuum (50 Pa) with dc bias=20 V.

3.2 Hysteresis characteristics

All four resonators were tested in order to analyze the hysteresis characteristics during upsweep and downsweep of the frequency. Fig. 3 shows frequency response curves of Res A under different excitation scenarios. Here Fig. 3a shows the resonator response in the air while varying dc bias from 12.9 V to 87 V with constant ac amplitude of 1 V. Q was calculated as 93 at dc bias=87 V and ac amplitude=1 V. It is clear from the shift in resonance frequency that the resonator exhibits spring-hardening effect. However in vacuum at 50 Pa, this effect is more pronounced while varying dc bias from 5 V to 25 V with constant ac amplitude of 105 mV as shown in Fig. 3b. In vacuum, slide-film damping between the fingers [10] and overall motional resistance against air molecules is lowered which results in a high Q factor. High Q factor and addition of third-order vibration pull frequency response to the right as the springs harden. At a specific value of the frequency during upsweep, the device can not maintain the high amplitude as it becomes unstable, and begins to vibrate at a lower amplitude in order to sustain the

DOI: 10.1587/elex.8.291
Received January 26, 2011
Accepted February 01, 2011
Published March 10, 2011

oscillations. The full nature of the hysteresis is revealed during upsweep and downsweep of the excitation frequency at dc bias=20 V and ac excitation amplitude=105 mV as shown in Fig. 3c. Based on this response, we can observe that for a given frequency value within the hysterectic region, two stable vibration amplitude states exist. Note that while switching states from high to low amplitude during upsweep and low to high amplitude during downsweep, the response shows slight ringing at the end points. This suggests that the device takes longer to settle to a stable amplitude due to low damping. Improving measurement accuracy in the instrument tends to lower this ringing effect. Fig. 3d shows the response during upsweep while increasing ac excitation amplitude from 55 mV to 305 mV at dc bias=20 V. As expected the response bends right with an increase in ac amplitude. At 305 mV, the resonance curve shows a clear transition from bending to a continuation of the resonance in higher vibration amplitude state before becoming unstable at a specific frequency. Flattening of the imaginary part in this region indicates almost constant change in capacitance. Note that this behavior was captured by performing a slow sweep. During fast sweep, the oscillations at the same excitation amplitude tend to settle into low amplitude very quickly and the hysteresis does not extend further. The response shown in Fig. 3d reappears during fast sweep only after increasing the excitation amplitude or decreasing the pressure. For example, when lowering pressure from 80 Pa to 20 Pa while keeping dc bias at 20 V and ac excitation amplitude 205 mV, the device exhibits similar response during upsweep. During downsweep in both cases, the jump point stays at the same value. The extension of hysteresis was also observed in Res B, Res C, and Res D. For identical values of pressure, dc bias, and ac amplitude, the approximate widths of the hysteresis for the four resonators were calculated as 73 Hz for Res A, 165 Hz for Res B, 216 Hz for Res C, and 42 Hz for Res D. It was observed that the presence and extension of hysteresis can be seen more accurately in vacuum; a change the ac excitation voltage does not quite show hysteresis in the air due to high damping. In an ongoing research, synchronized behavior of the resonators with different hysteresis widths, different individual resonance frequencies, and different Q factors is currently being investigated. Additionally it is worth noting that a single resonator can be switched more conveniently between two vibration states at a fixed frequency in the extended hysteresis region.

3.2.1 Mechanism behind extended hysteresis

Inner beams shown in Fig. 4a develop higher modes of vibration due to high compressive force experienced during peak resonance to maintain equilibrium; the truss can only partially remove the high tensile force present during peak resonance. This can cause spring-hardening effect. The ratio of outer beam spring constant to inner beam spring constant is 1.27. Because the outer beams are stiffer than the inner beams, they tend to compress less during peak resonance displacement. This type of nonuniform stress distribution can further harden the springs. Also note that in a symmetrical set of folded flexures containing four inner-outer beam pairs, force applied to

DOI: 10.1587/elex.8.291
Received January 26, 2011
Accepted February 01, 2011
Published March 10, 2011

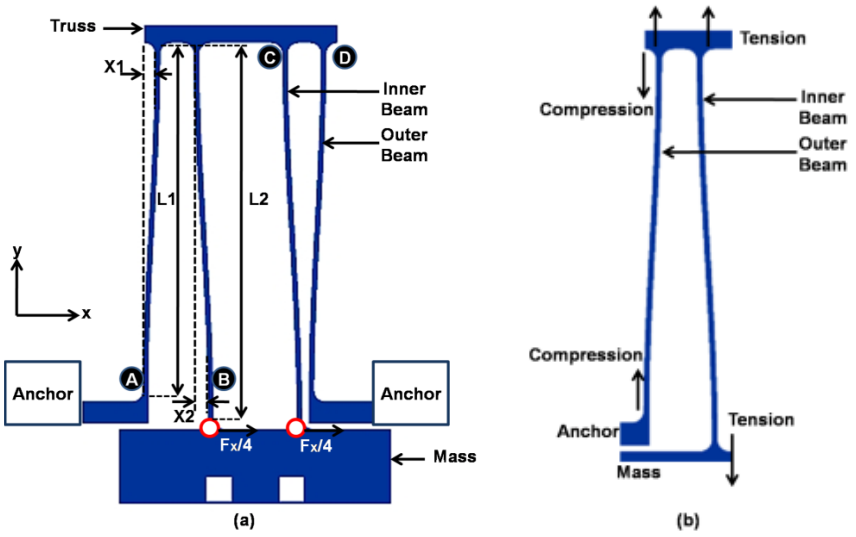

Fig. 4. Possible causes for the hard-spring effect and extension of hysteresis: (a) outer beams are stiffer than inner beams due to L1<L2 which makes the displacements X1 and X2 different at peak resonance. Also note the differences between distances A–B and C–D, and (b) compressive stress on the outer beam is lower whereas the tensile stress in the inner beam is higher.

each inner-outer beam pair is $F_x/4$, where F_x is the total applied force on the mass. Here the beams are not located at the same distance from each other on the truss which makes the applied force in a given inner-outer beam pair unequal during peak resonance displacement. This causes asymmetric expansion and contraction of the folded beams creating unequal distances denoted by A-B and C-D in Fig. 4a. Therefore the two factors, the location of the four beams on the truss and the ratio between the outer-inner beams in a given pair, can cause the mass to sustain the high amplitude state during peak resonance displacement.

4 Conclusion

In this paper, a MEMS resonator with extended hysteresis was reported. An increase in dc bias value tends to increase vibration amplitude but not necessarily extend the hysteresis. At high ac voltage and low pressure extension of hysteresis occurs in all four resonators with different resonance frequencies on separate dies. This indicates that the design of the structure along with specific excitation conditions are responsible for such a behavior. This resonator can be utilized in a number of applications such as filters and as wide bandwidth resonator within the hysteresis region.

Acknowledgments

This work was supported in part by Global Center of Excellence (GCOE) program at Kyoto University, Kyoto Environmental Nanotechnology Clus-

DOI: 10.1587/elex.8.291
Received January 26, 2011
Accepted February 01, 2011
Published March 10, 2011

ter, Regional Innovation Cluster Program 2010, and Ministry of Education, Culture, Sports, Science and Technology (MEXT). The authors also wish to thank Mr. Hiroyuki Tokusaki, Dr. Toshiyuki Tsuchiya, and Dr. Osamu Tabata (Department of Micro Engineering, Kyoto University).

DOI: 10.1587/elex.8.291
Received January 26, 2011
Accepted February 01, 2011
Published March 10, 2011